Arab Journal of Nuclear Sciences and Applications

Web site: ajnsa.journals.ekb.eg

(ESNSA)

Creep Behavior of β Cu-Zn Alloys

Mohammed A.Z., Abd El-Aziz El.Z., Attia A.M, and Mahmoud O.F.,
Department of Physics, Faculty of Science, Zagazig University, Zagazig, Egypt.

Transient creep tests are performed under constant stress conditions at temperatures ranging from 533 to 653° K for Cu-38wt%Zn, and Cu-38wt%Zn-2wt% Pb samples. The transient creep is described by $\xi_{tr} = \beta\, t^n$, where ξ_{tr} and t are the transient creep strain and time respectively. However, the parameters n, β are calculated, and the activation energy of the transient creep shows two regions for both alloys at low and high temperatures. Also, the activation energy was determined to clarify the controlling mechanism. At low temperature rang (513-633°k), the strain rate sensitivity parameter m has values (0.247-0.174) while its values at high temperatures ranging from (0.192 up to 0.263) at 653°K. These values give an indication that dislocation glide is probably an operating mechanism in grain boundary diffusion. Also, the change of microstructure grain size, microhardness, and stress-strain behavior have been studied.

Keywords: Transient creep, Cu-Zn-Pb, Lattice-diffusion, Dislocations

Introduction

The effects of microstructure changes and the mechanical properties have been studied for many years in great detail on numerous types of metallic materials. Also, many studies [1-7] have been conducted on nonferrous alloys such as brass alloys [8-12]. The effect of dislocation substructure on fatigue crack propagation (FCP) behavior in copper and α- brass was also studied [13]. However, during the transient creep, deformation could be presented by the equation [14]:

$$\xi_{tr} = \beta\, t^n \tag{1}$$

Where ξ_{tr} and n are the transient creep rate, and stress exponent, respectively. The parameter β is the transient creep parameter and was calculated from:

$$\text{Ln}\,\beta = \frac{\ln t_2 \ln \xi_{tr_1} - \ln t_1 \ln \xi_{tr_2}}{\ln t_2 - \ln t_1} \tag{2}$$

The parameter β was found to depend on the strain rate of the steady state creep (ξ'_{st}) through the relation [5]:

$$\beta = \beta_o\,(\xi'_{st}) \tag{3}$$

Where β_o is constant and γ depends on the experimental conditions. The effect of Pb addition reduces the grain size of the binary Cu-Zn from 30 to 20, 17, and 15 μm in alloys containing 2wt%Pb at 593, 613, 633, 653°K, respectively. To elucidate the grain refinement mechanism, it is worth considering the micro hardness, and microstructure analysis of phases.

The aim of the present study is to investigate the characteristics and the structural properties of the transient creep for both Cu-Zn and Cu-Zn-Pb alloys, and to determine the dominant operating mechanism for the present two alloys.

Corresponding author: adel.zaki47@hotmail.com

Experimental

The materials used were Cu-38wt%Zn, and Cu-38wt%Zn-2wt%Pb alloys were prepared from high purity Cu, Zn, and Pb by the induction melting in a graphite crucible. After homogenization at 1123°K for 20 min, and water quenching, the quenched samples were swaged to wires of 0.8 mm diameter and 50 mm gauge length. All the samples annealed at 573°K for 4 hrs to eliminate the cold work introduced during swaging, and to stabilize the structure. The samples were crept under constant applied stresses. Creep tests were carried out in an improved manual creep machine described earlier [15, 16]. The accuracy of temperature measurements is of order of ±1 K. Strain measurement were done with an accuracy of ±1X10-5 m. Hardness tests were performed using a Vickers microhardness tester (HMV-2T, Shimadzu) with a testing load of 245.2 mN (0.025 Kg) for 15 S dwell at room temperature.

For metallographic observation, samples were mechanically ground with 500, 800, 1500, and 4000 sic abrasive papers and then polished with 0.05 μm Al_2O_3 polishing suspension.

After polishing, samples were etched in a solution of 20%H_2O_2 (3%)-40% NH_4OH (conc.)-40% H_2O. Microstructural observation was carried out using an optical microscope (OM-Nekon) and a scanning electron microscope (SEM, JSM, 6500E, Jeol). Microstructures of the samples were analyzed using a SEM- wavelength dispersive spectroscope (FBSD) analysis; tensile tests were performed using the universal testing machine described previously by the author [15, 16] with a strain rate of 5X10-4 S-1

Results and Discussions

Transient Creep Curves

Fig.1 (a, b) Shows the creep behavior as a plot of ln ξ_{tr} against ln t for the present two alloys that were studied using different applied stresses at different working temperatures from 573 to 653 °K in steps of 20° K. The transient creep parameters n and β were calculated from Equ. (1). Also, the parameter β was calculated from Equ.(2), the exponent (n) was calculated from the slopes of the lines in Fig.1, and was found to have values ranging from (2.00 to 2.33) for Cu-38wt%Zn alloy, and from (1.54 to 1.99) for Cu-38wt%Zn-2wt%Pb alloy. The parameter β was found to

exhibit values ranging from (8.36 - 26.26) 10 -3 for Cu-Zn alloy, and from (3.35 - 9.45) 10-5 for Cu-Zn-Pb alloy. Fig. 2(a, b) demonstrates the temperature dependence of n and β for both alloys under the experimental conditions considered above. However, the activation energy of the transient creep Qtr was calculated from:

$$\xi_{tr} = \xi_o + t^n \exp(-Q_{tr}/kT) \qquad (4)$$

Where ξ_o is the instantaneous strain, Qtr is the activating energy, and T is the working temperature. Necking and Fracture of the sample does not occur and thus, there should not be a third stage of the curve, as would be observed in an ordinary tensile creep test. However, our creep curves exhibit an accelerated creep stage after the secondary creep region. This may be indicative of a phase transformation which takes place in the weaker phase. In the present study the phase transformation for both alloys takes place at 613 °K in excellent agreement with the phase diagram [17]. The mutual solubility of Cu and Zn is altered leading to variations in the microstructure of the phases α and β- phase due to the changes in their volume fractions [18]. The enhancement of transient creep of both alloys may be attributed to the formation of new dislocation sources during the rearrangement of dislocations in the dislocation network of the β phase during phase transformation. Moreover, the enhancement of the transient creep by increasing the applied stress can be attributed to the superposition of the applied stress on the internal stress established during transformation caused by the difference in the specific volume of the product and parent phases.

In the ternary Cu-Zn-Pb alloy the increased number of phases or more precise on the increased number of the interfaces there will be Cu/Zn, Zn/Pb, Cu/Pb, Cu/Cu, Zn/Zn, and Pb/Pb phase boundaries, while in binary Cu-Zn alloy, there will be three interfaces only. Therefore, the Cu-Zn-Pb alloys show enhanced transient creep properties higher than those of the binary Cu-Zn alloys as summarized in Table (1).

Finally, the presence of both α and β-phase obstacles affect the distance that dislocations glide between these obstacles and the forces that cause them to climb. At phase transformation temperature coherent interface α/β acts as a one - way valve, allowing dislocations to move freely from α-phase into β-phase, but not vice versa.

Consequently, the recovered alloy is rich in dislocations in the β-phase, whereas the α-phase is almost clear of dislocations. Also, the characteristics of the transient creep are largely (to big extent) altered by addition of third element (Pb). Moreover, it is clear from Fig. (2) that the transient creep parameter n and β may be used to identify the dominant creep deformation mechanisms under specific stress and temperatures. However, the previous Table shows variations of n and β parameters with a change of chemical compositions of the present alloys and the related transient creep characteristics of both binary and ternary Cu-Zn-Pb alloys. The activation energy Q_{tr} (KJ mol^{-1}) was calculated.

Therefore, the present results give an evidence for the existence of two types of creep behavior in Cu-Zn alloy. Both n and Q_{tr} are material parameters that may be used to identify the dominant creep deformation mechanism in a specific range of stress and temperature. According to the theory of dislocation climb controlled creep, the stress exponent has the value of Table (1) and the activation energy has the value of the activation energy of the lattice self-diffusion [20-24]. However, the theory of dislocation viscous glide leads to stress exponent (n) of 2 at high temperatures and high values for low temperatures. However, the present results support the idea that the controlling process during the transient creep in β Cu-Zn alloys is not a single process, there is a transition in creep behavior from one controlled process with activation energy 25.6 KJ/mole. This transition can be reflected either as change in the stress exponent or as a change in the different parameters of transient creep. In the present alloys, there are two different creep mechanisms operating in the high and low stress regions. Fig. (3) Shows the relationship between ln β versus ln ξ´st at high and low temperatures. On the other hand, Fig. (4) shows the relation between ln βand 1000/T for different applied stresses for (a) Cu-38wt%Zn and (b) Cu-38wt%Zn-2wt%Pb alloys.
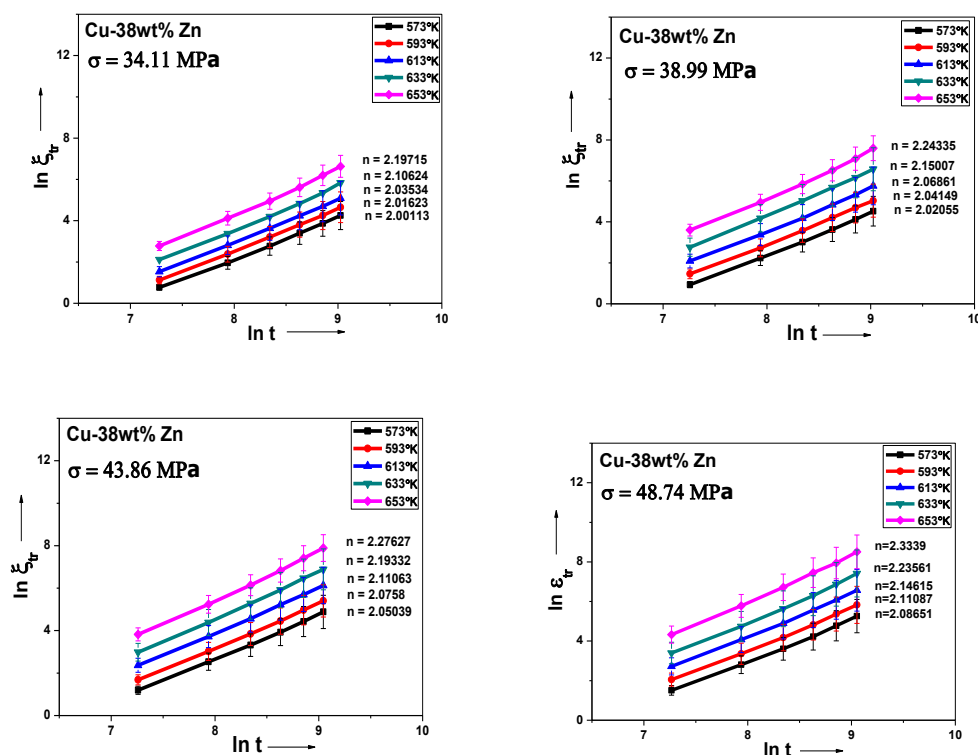

Fig. (1-a): Shows a relation between ln ζ_{tr} and ln t for Cu-38wt%Zn alloy at different applied stresses and various temperatures
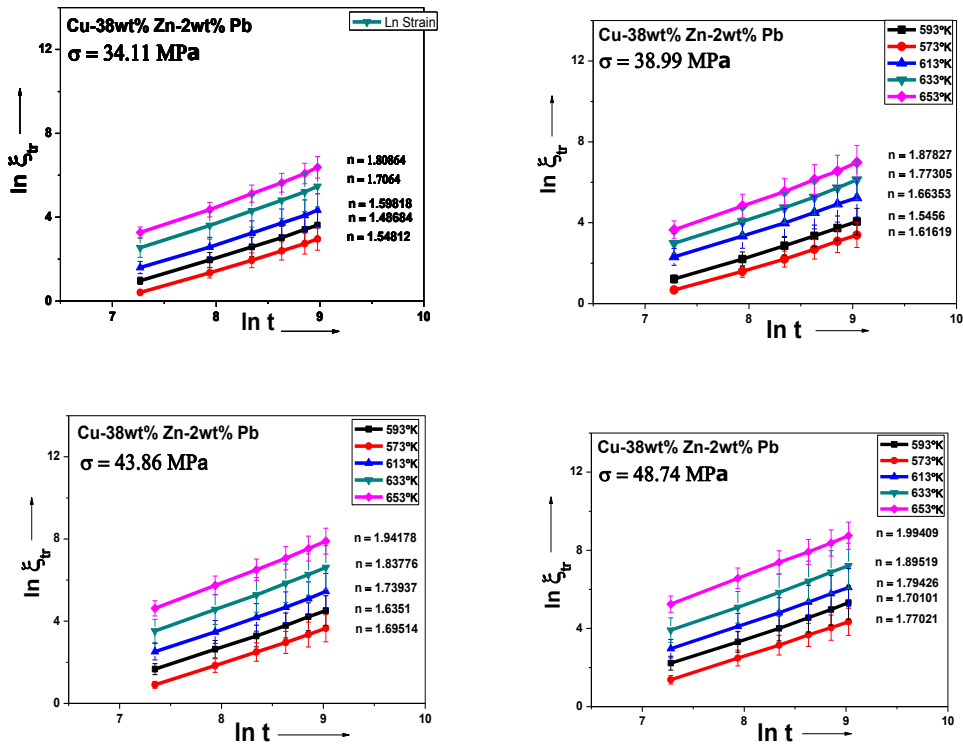
Fig. (1-b): Shows a relation between ln ζ$_{tr}$ and ln t for Cu-38wt%Zn-2wt%Pb alloy at different applied stresses and various temperatures
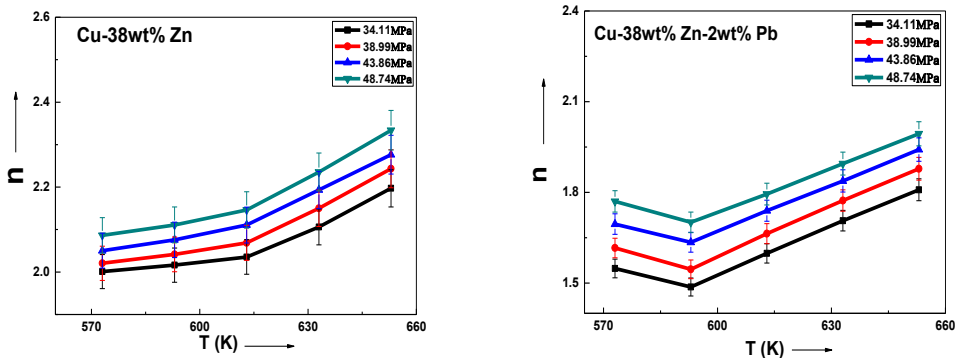

Fig. (2-a): The dependence of the exponent (n) on the working temperatures at different applied stresses for   a) Cu-38wt%Zn and b) Cu-38wt%Zn-2wt%Pb alloys
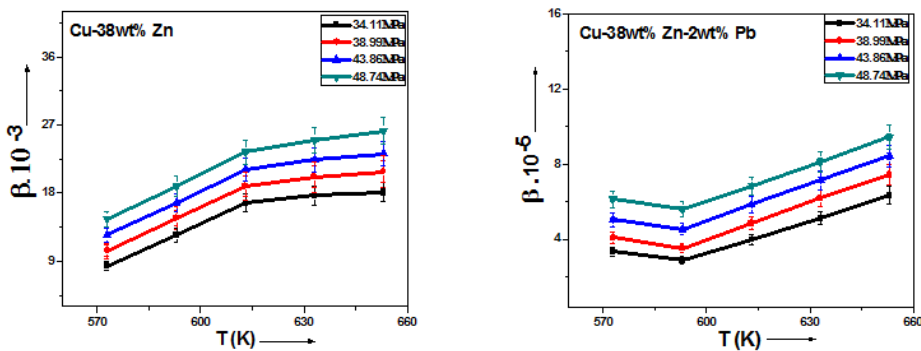

Fig. (2-b): The dependence of the parameter (β) on the working temperatures at different applied stresses for   a) Cu-38wt%Zn and b) Cu-38wt%Zn-2wt%Pb alloys

Table (1): The enhanced transient creep properties of Cu-38%Zn and Cu-38%Zn-2%Pb alloys

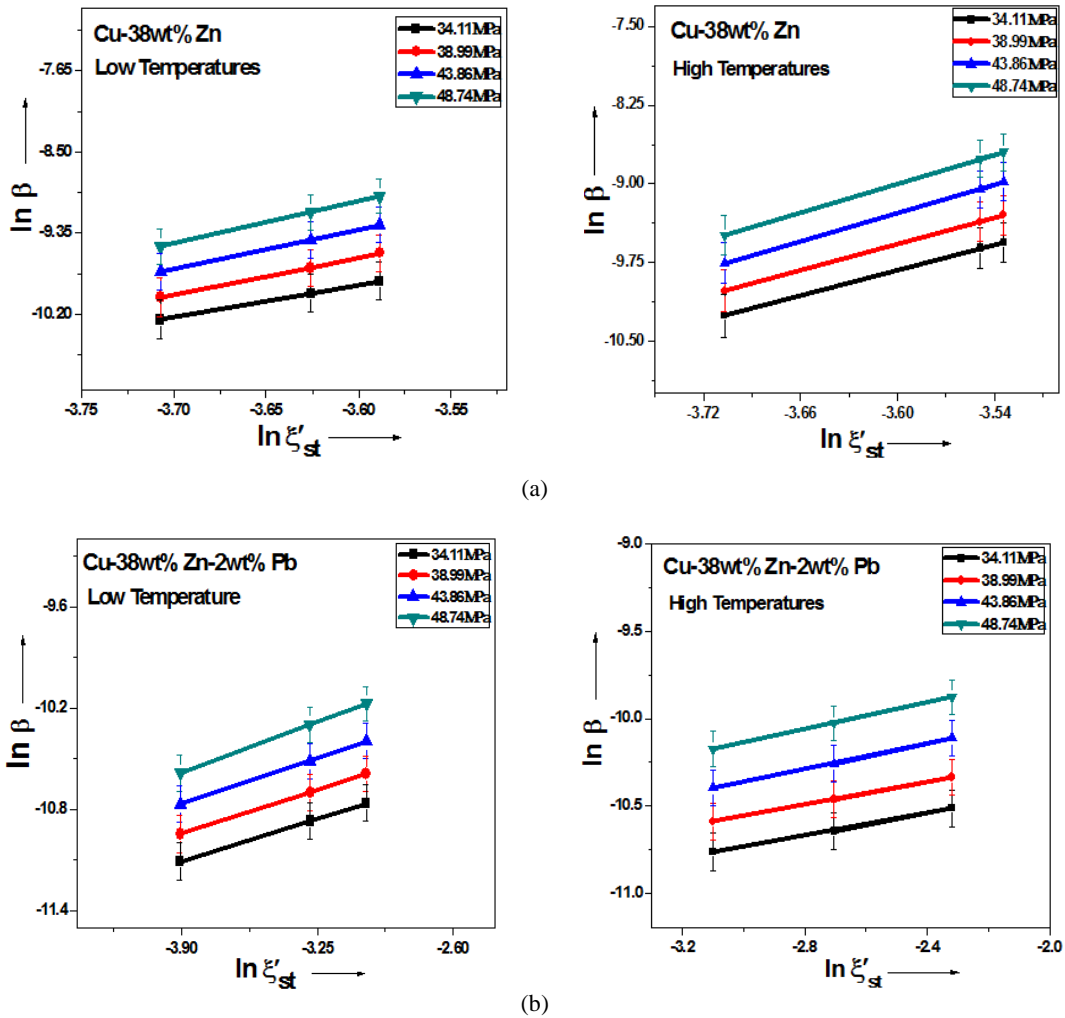| Materials	Exponent (n)	Parameter β	Activation Energy Q_{tr} KJ/mole	Grain Diameter (μm)
1.Cu-38wt%Zn	2.00 – 2.33	$(8.36–26.26)10^{-3}$	25.25-25.78	9.46-15.38
2.Cu-38wt%Zn-2wt%Pb	1.54 – 1.99	$(3.35–9.45)10^{-5}$	16-18	8.2-13.07

(a)

(b)

Fig. (3): The variation of the transient creep parameter β with the steady state creep ξ'_{st} for different applied stresses for a) Cu-38wt%Zn and b) Cu-38wt%Zn-2wt%pb alloys
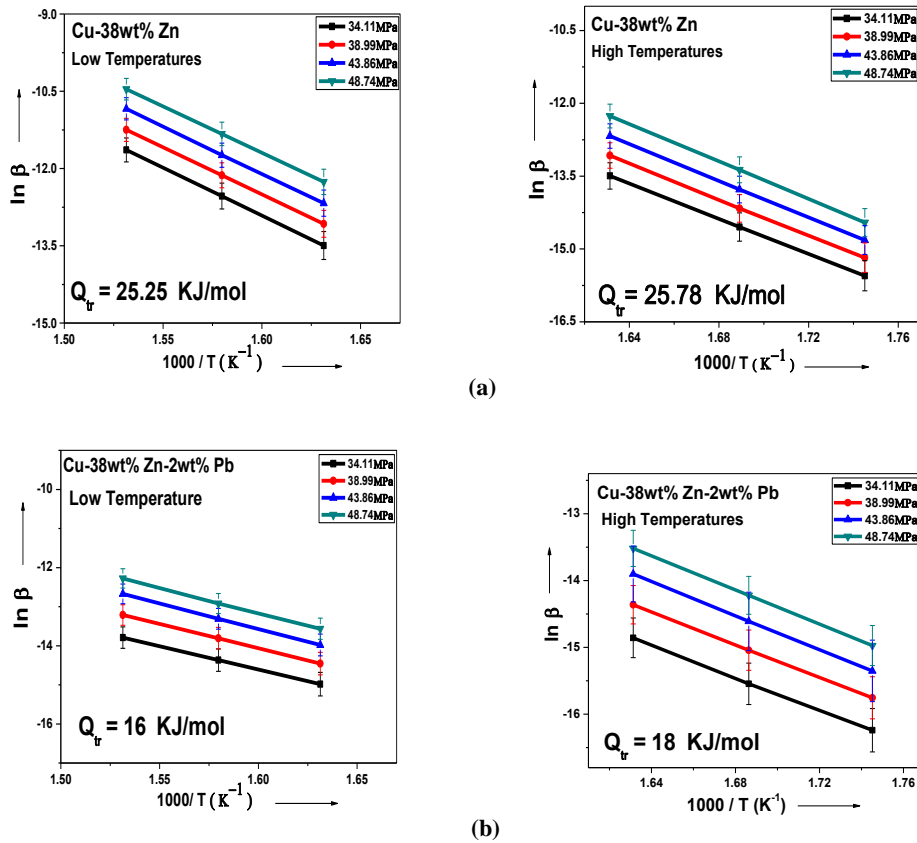
Fig. (4): Relation between ln β and 1000/T for different applied stresses for a) Cu-38wt%Zn and b) Cu-38wt%Zn-2wt%Pb alloys

The role of the grain size and microstructure
It is well-known that a reduction in grain size leads to an increase in yield stress of a material per the well-established Hall-Petch relation:

$$\sigma_y = \sigma_{\circ} + K_y \, d^{-1/2} \qquad (5)$$

Where σ_y is the yield strength, $\sigma_{\circ}$ is the friction stress opposing dislocation motion, K_y is the dislocation locking term, and d is the grain size. However, it was more recently reported [20] that the increase in yield strength with grain refinement in excellent agreement with the present results. Fig. 5 (a, b, c, and d) shows the equiaxed grains for both α and β as two phase structure of β- brass of Cu-38%Zn. Optical micrographs, β phase was fragmented as shown in Fig. (5 a), but α phase didn't experience any deformation or dislocations. Fig. (5 b) shows rearrangement of the affected boundaries (BC, CD, IH, and HG) in order to remove the unstable re-entrant angles (at C and H) as in the schematic illustration of subgrain

coalescence by subgrain rotation [23-25]. Migration of high angle boundaries which occurs during the growth angle of primary recrystallization. Refine of grains takes place after adding (2wt% pb), the grain size will be around (8.2-13.07) μm instead of the binary β –brass (about 9.46 μm up to 15.38 μm). Fig (5 c) shows the mechanical twinning and recrystallization of grains at moderate transformation with sub-grains for a sample heated at 850˚c/20 min, and quenched in water then heated up to 360 ˚c for 49 min. Fig. 5(d) shows twin and slip plans, the thickness of the twin layer λ and separated by Δ as shown in the schematic diagram below. Also, Fig. (6) shows optical and scanning electron micrographs of Cu-38wtZn-2wt%Pb ternary alloy with grain boundaries with σ ≈ μm thick, and fine grains with precipitations of intermetallic compound (7 μm) as shown in the scanning electron micrograph Fig .(6 e). Optical microstructures of the alloys, shown in Fig. 5(a-c), are indicative of bainitic structure. All structures had α-β duplex phase with grain sizes in

the range from 9.46-15.38 µm for the binary Cu-38wt%Zn and within 8.2-13.07 µm for the ternary Cu-38wt%Zn-2wt%Pb alloys, have an equiaxed shape under the applied stress the grains elongated and then recovered again before deformation. After adding lead to the binary Cu-38wt%Zn, the grain size refined and gives its minimum at or near 613˚K.

Microhardness
Microhardness measurements are plotted against aging temperature at 280, 300, 320, 340, 360, and 380°c for both the binary Cu-38wt%Zn, and the ternary Cu-38wt%Zn-2wt%Pb, respectively Fig.7(a, b): It can be noticed that the microhardness reached the minimum value at or near 613˚K. This microhardness evolution is attributed to the change of the volume fractions of α and β-phases as a function in the aging temperatures. It was reported [20] that β phase is harder than α-phase; the results of the present study confirmed the reported results. Also, the present results show that the microstructure reveals duplex-phase structure from α and β-phases.

Finally, the structure of the present brass shows a dominant α-phase in the range 320-340˚c as shown in the Cu-Zn phase diagram bearing in mind that microhardness of the α-phases is less than that of the β-phases as shown in Fig.(7 a). However, the average microhardness of the α and β-phases for the present ternary alloy (Cu-38wt%Zn-2wt%Pb) were 76 HV and 108.5 HV, respectively. These values are higher by 15% for α-phase and 19% for β-phase, respectively (α-phase microhardness, about 70 HV and β-phase 96 HV) for the binary Cu-Zn system. The results of the present work are in accordance with the data published by Haruhiko etal [10]. For Cu-40wt%Zn alloy (α-phase microhardness≈100 HV and microhardness for β-phase was 144 HV). The difference between our results and Haruchico et al. was attributed to the difference in Zinc concentration and the effect of Pb which causes a pinning effect of Pb ($Cu_{1-X}-Zn_X$) precipitates at the grain boundaries, and refined the grain size as mentioned before.

X-ray diffraction
Fig. (8) shows large peaks due to the α-phase and to the β-phase, and small peak due to Pb in the ternary brass alloys. Also, the width of all of the diffraction peaks after formation of bainite broaden, which indicates that the grains are fragmented or refined after adding 2wt% Pb and after aging the diffraction peaks have thinned. As a result for lowering the internal stress. Fig. (8) reveals that all of the α and β phases and Pb ($Cu_{1-X}-Zn_X$) small peaks all co-exist in the alloys. These phases will be confirmed by the qualitative morphological characterization by SEM/EDX analysis. Also, the locations of the peaks at 2Θ do not change, but its height has changed only and the volume fractions of both phases changed too.

Elemental analysis (EDX)
Fig. 7 (a, b) shows the microhardness of the present alloys and Fig. (7 c) shows the corresponding EDS analysis of some locations on both α and β-phase at different aging temperatures. However, the chemical compositions of different phases are listed in Table (2).

Fig. (7 c) Shows cross-sectional back scatter electron (BSE) microanalysis of the present two alloys and corresponding EDS analysis of some locations. The microstructure of the present alloys shows two phase structure α and β phase co-existed with different volume fractions changes of the working temperatures. Also, the addition of Pb to the binary Cu-Zn refine the grain size and forms the intermetallic compound (IMC) Pb ($Cu_{1-X}-Zn_X$) which makes a pinning through the grain boundaries. The structure of the α-phase is a lamellar structure with the interlamellar spacing ≈ 13 µm as an average value within the working temperatures and increases with increasing the temperatures. The corresponding chemical compositions are presented in Table (2) at positions A, B, and F respectively. The analysis of the phases under consideration is illustrated in Table (2).

Stress-strain behavior of β-brass
It becomes apparent that the superplasticity of the two alloys has much altered by the amount of Zn added, and, the other alloying elements (Pb, Sn, Sb, and Al or…etc). The fact that the Cu-38wt%Zn-2wt%Pb alloys show a higher elongation and lower flow stress alloys than the other Cu-38wt%Zn binary alloys is quite remarkable and indicates that the ternary alloys (Cu-38wt%Zn-2wt%Pb) are promising . The microstructure of our present two alloys were uniform, stable and of finer grain size as shown in

Fig. (5, 6) Also, in the binary alloy possesses a large equiaxed grains and lower microhardness with common minimum at or near to 613° K as shown in Fig .6(a). On the other hand, for the ternary alloy Cu-38wt%Zn-2wt%Pb contains cavities, microcracks, and small or grain size with a higher microhardness as shown in Fig. 6(b). Fig. 9(a, b) shows the tensile behavior of the two alloys at room temperature and a strain rate of 6x 10^{-5} sec^{-1}.The two alloys show a reasonable ultimate tensile strength for the binary alloy (UTS): 320 MPa and for the ternary alloys its (UTS): 375 MPa which shows a higher ductility. The presence of Pb ($Cu_{1-x} Zn_x$) intermetallic compound in the matrix was most likely the cause of the observed increase in the strength of the Cu-38wt%Zn-2wt% Pb alloy.

This may tend to increase the tensile resistance of the ternary alloy. It can be concluded that the ternary alloy exhibits improvement in both strength and ductility as compared to the binary alloy. Table (3) shows a summary of microstructure and mechanical characteristic of (a) Cu-38%Zn and (b) Cu-38wt%Zn-2wt%Pb samples [10].

From Table (3), it can be concluded that the high strengthening mechanism of the brass alloy was mainly attributed to the grain refinement of both α and β phases by the pining effect of the fine Pb (Cu1-xZnx) precipitates. Also, this might be attributed to its inhibiting effect on grain growth [25].

(a)

(b)

(c)

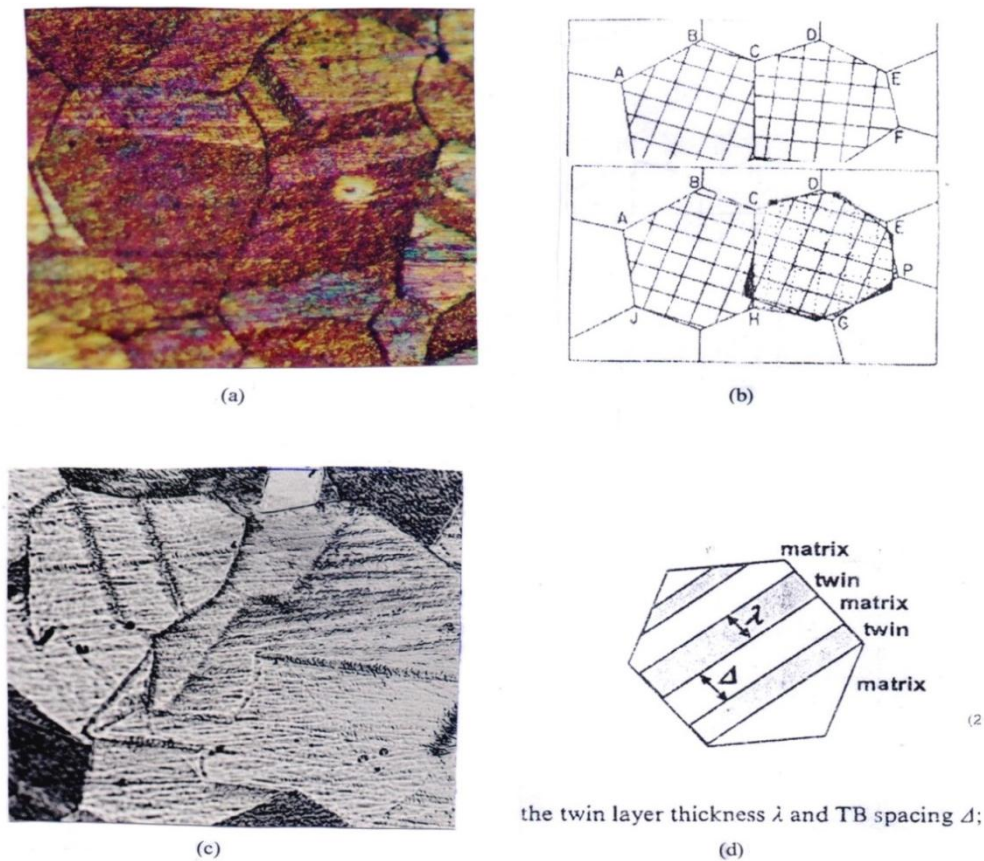the twin layer thickness λ and TB spacing $\varDelta$;

(d)

Fig.5 Grain size of Cu-38wt%Zn shows some crystalline defects

(a) Shows subgrain coalescence by subgrain rotation

(b) Schematic illustration of (a)

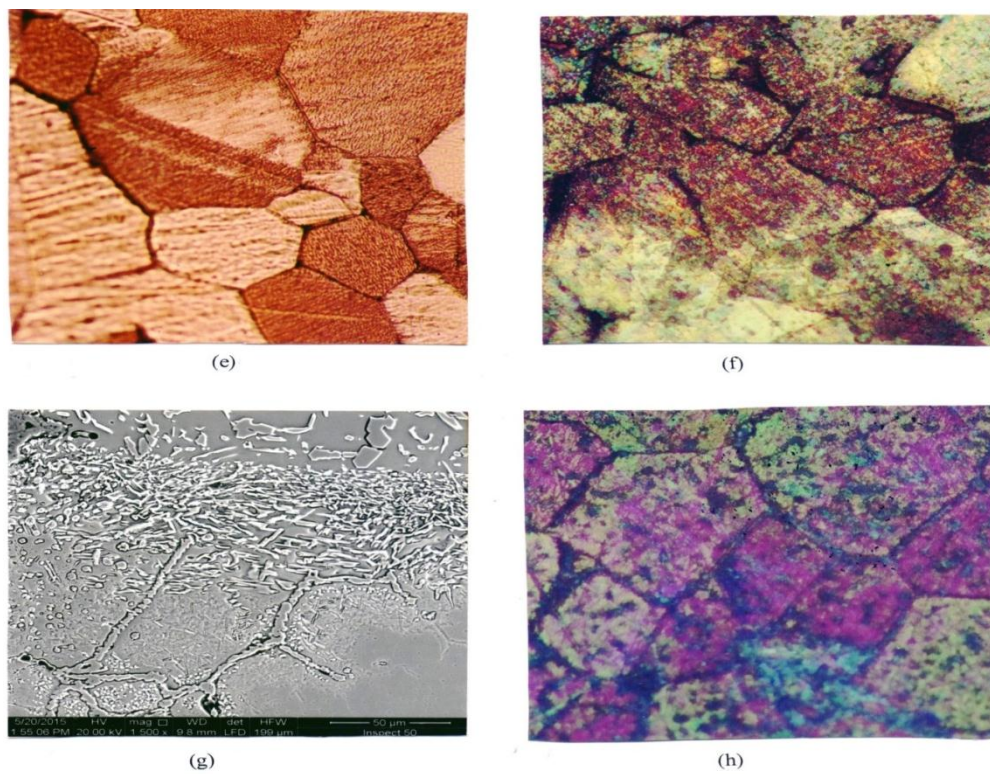(c) Twin layers (mechanical twining)

(d) Shows its schematic representation

Fig. 6 shows grain size of β-brass of Cu-38wt%Zn alloys

(e) α-βgrains with twining plane mirror

(f) Shows tearing in grain or fragment

(g) Scanning electron micrograph shows adjacent grains free from any precipitates

with coarse grain boundary

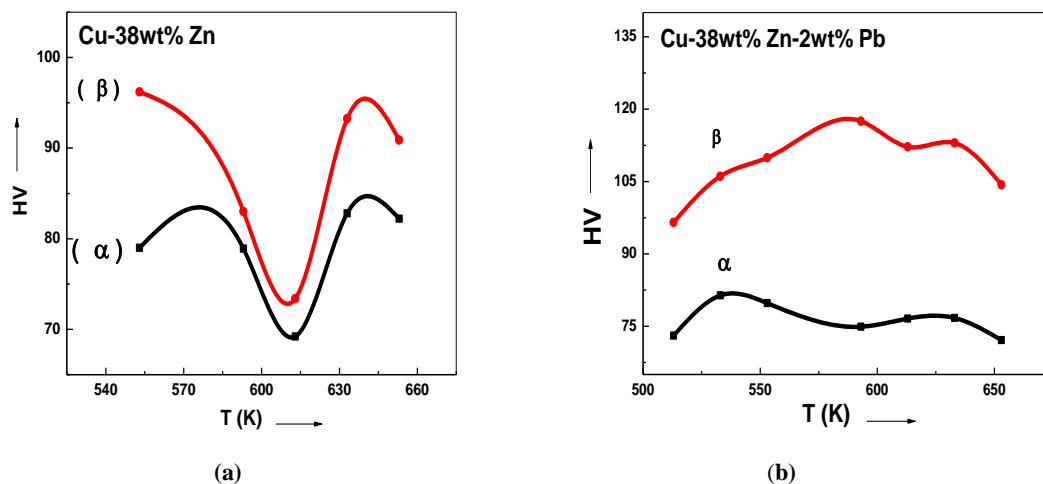(h) Grain size of Cu-38wt%Zn-2wt%Pb with dark coarse grain boundaries.

(a)   (b)

Fig. (7): the effect of the working temperatures upon the microhardness of both phases α and β for (a) Cu- 38wt%Zn and (b) Cu-38%Zn-2wt%Pb alloys
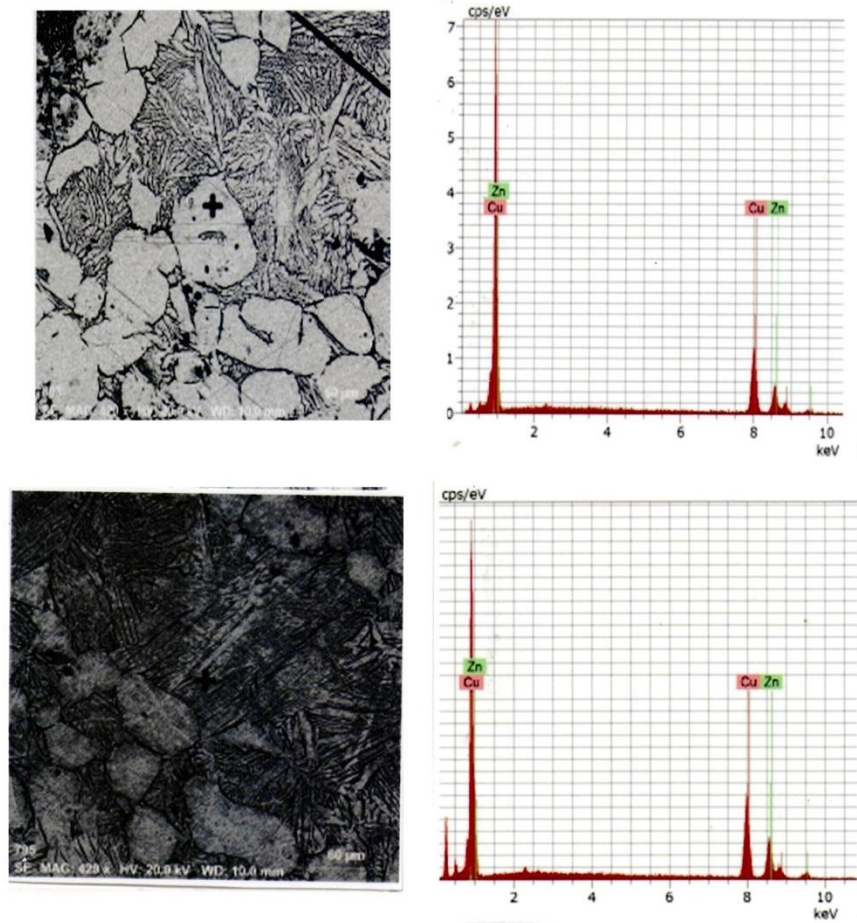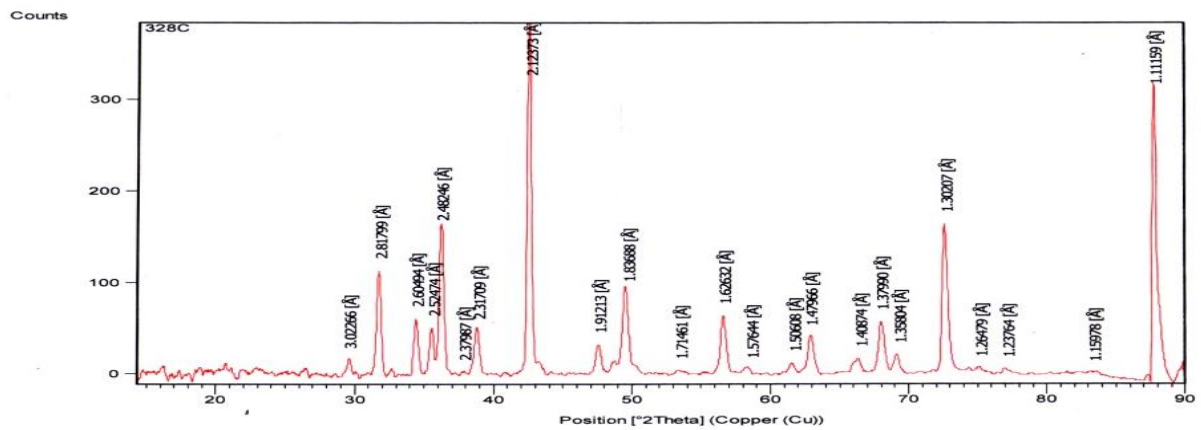
Fig. (7 c): SEM of binary Cu-Zn alloys shows the location of the beam and the corresponding X-ray microanalysis on β and α phases
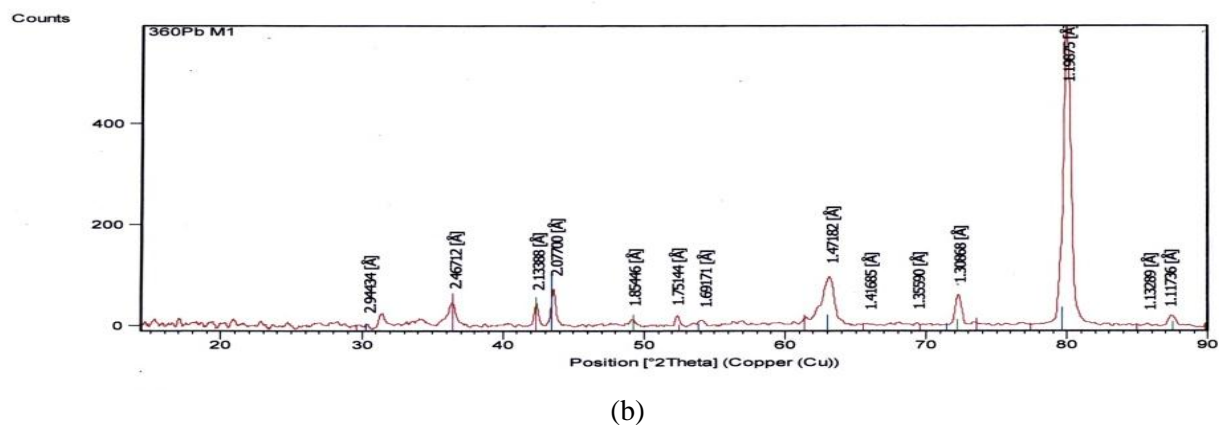

(a)

(b)

Fig. (8): X-ray diffraction peaks for two successive brass samples (a) Cu-38wt%Zn   and (b) Cu-38wt%zn-2wt%pb

Table 2: The chemical composition of different phases of Cu-38%Zn and Cu-38%Zn-2%Pb alloys

Temp. °c	Cu-38wt%Zn		Cu-38wt%Zn-2wt%Pb		
	Zn	Cu	Zn	Cu	Pb
553°K	35.65	64.35	38.47	59.01	2.52
573°K	37.14	62.86	36.11	61.28	2.61
593°K	36.76	63.24	36.55	60.87	2.58
613°K	35.20	64.80	36.77	61.12	2.11
633°K	33.48	66.52	36.79	60.50	2.71
653°K	36.63	63.37	35.82	61.45	2.73

Table (3): The microstructure and mechanical characteristic of (a) Cu-38%Zn and (b) Cu-38wt%Zn-2wt%Pb alloys

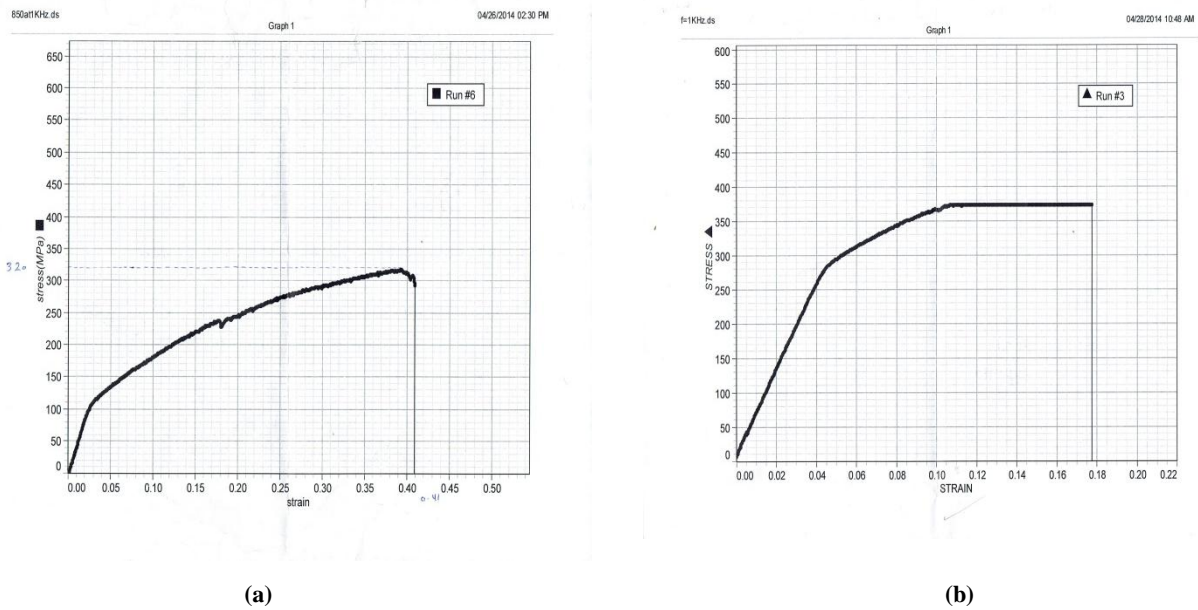| Samples	Average grain size (μm)	Hardness /Hr (β)	YS/ MPa	UTS/ MPa	Elongation
Cu-38%wtZn	9.46-15.38	96	60	320	27.5
Cu-38wt%Zn-2wt%Pb	8.2-13.07	108.5	65	375	37.5

(a)   (b)

Fig. 9 the stress-strain relationship for (a) Cu-Zn, and (b) Cu-Zn-Pb alloys. Both at room temperature and strain rate of $6*10^{-5}s^{-1}$

Conclusions

Tensile tests for Cu-38wt%Zn, and Cu-38wt%Zn-2wt%pb alloys were investigated. The effect of Pb on the microstructures and mechanical properties were studied too. Also, the effects of strain rate and microhardness on the mechanical properties were studied. Some useful results and conclusions are summarized below:

1. From the microstructure, the addition of lead refines the grain sizes of the binary Cu-Zn equiaxied grains into semi superplastic grains near to 15 μm with some air cavities.
2. Average yield strength (YS) and ultimate temperature (UTS) of the binary Cu-Zn, and the ternary Cu-Zn-pb alloys were 60 MPa , 65 MPa and 320 MPa, 375 MPa, respectively. These alloys exhibited YS and UTS that were 15% and 19% higher than conventional brass Cu-40Zn-pb alloy (α- phase microhardness). The ductility changes for the ternary are better than the binary alloy.
3. The microhardness, and gain sizes of the present two alloy shows a decrease with increasing temperature until near or at 613˚K (phase transformation temperature), and starts to increase with increasing temperature.

4. A significant improvement in the creep resistance of Cu-38%Zn alloy was observed due to the addition of 2wt%Pb.

References

1- Pantazopoulos G., J. Mater. Eng. Perform, Vol.11, (2002), pp.402-407.
2- Japan Copper and Brass Association, Base and Industrial Technology of Copper and Copper Alloys, in Japanese, (1994).
3- Garcia P., Rivera S., Palacios M., Belzunce J., Eng. Fail. Anal. Vol.17, (2012), pp.771-776.
4- Mahmoudi R., Eslami M., J. Mater Sci: Mater Electron Vol.22, (2011), pp.1168-1172.
5- Mahmoudi R., Eslami M., J. Mater Electron Vol.39, (2010), pp.2495-2502.
6- Kang N., Nahs K. Kangey S.J, J. Alloys and compounds, Vol.467, (2009), pp.246-250.
7- Jcm Li., Impression creep and other localized tests. Mater Sci. Eng. A Vol.322, (2002), pp.23-42.
8- Morris D.G, Morris M.A. Mater Sci. Eng. A Vol.23, (1997) pp.239-240.
9- Hirsh P.B., Progr Mater Sci, (1992), pp.36-63.
10- Atsumietal H., Materials Chemistry and Physics Vol.135, (2012)pp.554-562.

11- Nayyeri G., Mahmdi R., Mater. Sci. Eng. A Vol.527, (2010), pp.669-678.

12- Mohamed A.Z, Saker M.S., Abdel-Daiem A.M., Shehab M., Phy. Stat. Sol. (a), Vol.133, (1992), p.51.

13- Hitoshi I., Kazuhiko Y., Metal. Mater. Trans. A,Vol.10, (1979).

14- Friedel, Dislocation, Brass, London, (1964), p.304.

15- El-Daly A.A, Mohammad A.Z., Fawzy A., El-Taher A.M.; Mater Sci, and Engineering A Vol.528, (2011), pp.1055-1062.

16- El-Daly A.A, Fawzy A., Mohammad A.Z., J. Alloys and Compounds, Vol.509, (2011), pp.4574-4582.

17- Hansen M. and Andreko K., Constitution of Binary Alloys, Mc.Graw, Hill publ. co, NewYork, (1958), p.1217.

18- Atsumi H., Imai H., Li S., Knodoh K., Mater Sci. and Engi. A. Vol.529, (2011), pp.275-281.

19- Gargetal R., Materials Science and Engineering A Vol.527, (2010), pp.4582-4592.

20- Li S., Imai H., Astumi H., Kondoh K., J. Alloys and compounds. Vol.493, (2010), pp.128-133.

21- Liu Z.Y et al., Materials Science and Engineering A Vol.242, (1998), pp.137-140.

22- El-Daly A.A., phys. Stat, sol. (a), Vol (200) 2, (2003), pp.333-338.

23- Baker I., Yang Y., Mater. Sci. Eng. A Vol.109, (1997), pp.239-240.

24- Lee K.A. et al., J. Acta Materials ,Vol.52, (2004), pp.2913-2922.

25- Moles M.D.C, Davies G.J., Metal Sci. Vol.314, (1976).